Earth And Planetary Science Letters
May 2018, Volume 490 Pages 143-150
http://dx.doi.org/10.1016/j.epsl.2018.03.017
http://archimer.ifremer.fr/doc/00434/54567/

Continental-scale transport of sediments by the Baltic Ice Stream elucidated by coupled grain size and Nd provenance analyses

Boswell Steven [1, 2, *], Toucanne Samuel [3], Creyts Timothy T. [1], Hemming Sidney R. [1, 2]

[1] Lamont Doherty Earth Observ, Palisades, NY USA.
[2] Columbia Univ, Dept Earth & Environm Sci, New York, NY 10025 USA.
[3] Inst Francais Rech Exploitat Mer IFREMER, Unite Rech Geosci Marines, Issy Les Moulineaux, France.

* Corresponding author : Steven Boswell, email address : boswell@ldeo.columbia.edu

Abstract :

We introduce a methodology for determining the transport distance of subglacially comminuted and entrained sediments. We pilot this method on sediments from the terminal margin of the Baltic Ice Stream, the largest ice stream of the Fennoscandian Ice Sheet during the Last Glacial Maximum. A strong correlation (R2 = 0.83) between the εNd and latitudes of circum-Baltic river sediments enables us to use εNd as a calibrated measure of distance. The proportion of subglacially transported sediments in a sample is estimated from grain size ratios in the silt fraction (<63 μm). Coupled εNd and grain size analyses reveal a common erosion source for the Baltic Ice Stream sediments located near the Åland sill, more than 850 km upstream from the terminal moraines. This result is in agreement with both numerical modeling and geomorphological investigations of Fennoscandinavian erosion, and is consistent with rapid ice flow into the Baltic basins prior to the Last Glacial Maximum. The methodology introduced here could be used to infer the distances of glacigenic sediment transport from Late Pleistocene and earlier glaciations.

Highlights

► A new method for estimating the transport distance of fine subglacial sediments. ► Fine sediments from the southern FIS margin were transported more than 850 km. ► Continental-scale transport of silts is consistent with modeling and till removal.

Keywords : Fennoscandian Ice Sheet, Baltic Ice Stream, provenance, epsilon Nd, grain size, EMMA

1. Introduction

Ice streams act as the arteries of ice sheets (Bennett, 2003), delivering large quantities of ice from interior regions of positive mass balance to the margins (i.e., Rignot et al., 2008). Ice streams flow via internal ice deformation, sliding of basal ice across the bed, and the deformation of subglacial sediments (Cuffey and Paterson, 2010). The transport of sediment provides an

important constraint on the basal conditions and processes beneath former ice streams (e.g., Clark, 1987; Houmark-Nielsen et al., 1987; Kjær et al., 2003; Stokes et al., 2015).

The Baltic Ice Stream was the largest of the Fennoscandian Ice Sheet (FIS) ice streams (Hughes et al., 2016; Stroeven et al., 2016), flowing south into the topographic lows of the Bothnian and Baltic Sea basins (Fig. 1; Houmark-Nielsen, 1987; Kleman et al., 1997; Boulton et al., 2001; Patton et al., 2016). From the initiation of fast flow around 38-35 ka BP, the Baltic Ice Stream advanced and retreated over the Baltic Sea basin several times. The ice stream reached its southern terminus in Denmark, Germany, and Poland during the Last Glacial Maximum ca. 23 to 21 ka BP (LGM; Hughes et al., 2016; Toucanne et al., 2015).

Numerical modeling of the FIS suggests an area of high subglacial erosion between the central Bothnian and central Baltic Seas (Fig. 1; Patton et al., 2016). This zone of maximal erosion is consistent with a wide region of glacial scouring and till removal near the Åland sill (Kleman et al., 2008), and 41-60% of LGM boulder and gravel indicators in the southern Baltic correspond to this this erosion source (Overweel, 1977). The transport history of fine sediments by the Baltic Ice Stream, however, is less certain.

Isotopic provenance, in which transported sediments are fingerprinted and referenced to the signatures of other rocks in the basin, provides a robust interpretation of the source of Baltic Ice Stream sediments (i.e., Toucanne et al., 2015). Isotope methods are particularly valuable for fine sediments, as petrographic identification is difficult at this scale.

In this study, we present a new method for discerning the distance of fine sediment transport by ice sheets. We pair the grain size distributions and εNd of glacigenic silts to identify sources for far-traveled and distally-sourced sediments. For sediments collected near the LGM terminus of the FIS in Denmark, Germany, and Poland, we document continental scale transport of the coarse silt fraction. Our reinterpretation of the glacigenic sediment εNd record in the

57 southern Baltic provides a convergence among geochemical, geomorphological, and numerical
58 model results of sediment sources and transport by the Baltic Ice Stream.
59
60 1.1 Provenance characterization of εNd in the Baltic Sea region
61
62 The origin of glacigenic sediments can be inferred from the Sm-Nd isotope system and
63 corresponding εNd values. εNd is the parts per ten thousand deviation of $^{143}Nd/^{144}Nd$ in a sample
64 from the chondritic uniform reservoir, or CHUR, where ^{143}Nd is the alpha decay product of ^{147}Sm.
65 Sm is less incompatible during mantle melting than Nd, and thus Nd is preferentially enriched in
66 the melts that separate from the mantle. Because the Sm/Nd ratio of continental crust is relatively
67 low and mostly uniform (Taylor and McLennan, 1985; Goldstein and Jacobsen, 1988), the εNd of
68 continental crust and its detritus becomes progressively more negative (non-radiogenic) with age
69 (e.g., Taylor and McLennan, 1985; McLennan and Hemming, 1992; Bayon et al., 2015). The εNd
70 of crustal material is typically unaffected by weathering, subsequent thermal events, or other forms
71 of alteration (Taylor and McLennan, 1985). Processes occurring during sediment transport do not
72 change the εNd of rock fragments, so the sources of glacigenic sediments deposited by the Baltic
73 Ice Stream can be ascertained from their εNd.
74 Because rivers integrate the sediments within their catchments, the εNd values of detrital
75 grains reflect the relative formation ages of constituent crust. The interpretation of these εNd
76 values (Soulet et al., 2013; Freslon et al., 2014; Toucanne et al., 2015) is consistent with the
77 bedrock geology of the Fennoscandian region (Fig. 1; Gaál and Gorbatschev, 1987; Gorbatschev
78 and Bogdanova, 1993). Archean bedrock (>2.5 Ga) lies to the north and east of the Gulf of Bothnia
79 in northern Finland and northwest Russia. Much of the remaining terrane in circum-Baltic
80 Fennoscandia (i.e., Sweden, Finland, and Denmark) is Paleoproterozoic in age (2.0 - 1.65 Ga),

with the youngest bedrock concentrated in Denmark and southwest Sweden. Fennoscandia was altered by both the Sveconorwegian-Grenville orogeny (1.2 - 0.9 Ga) and Caledonian orogeny (0.5 - 0.4 Ga), but these produced relatively little new continental crust in the region (e.g., Mykkeltveit et al., 1980; Gaál and Gorbatschev, 1987; Gorbatschev and Bogdanova, 1993). The relationship between river sediment εNd and regional outcrop geology is obscured in the southern and southeastern Baltic, however, by the extensive coverage of Phanerozoic sedimentary rocks (i.e., Winterhalter et al., 1981). Because the depositional ages of these sedimentary units do not necessarily reflect the formation ages of their constituent fragments, we rely on the εNd of the rivers that drain these terranes to rigorously fingerprint their crustal signatures.

1.2 Comminution

Subglacial sediments are crushed and abraded against the bedrock and other clasts by the flow of ice. This reduction of clasts to smaller fragments is termed comminution. The integrated effect of comminution leads to characteristic grain size distributions (e.g., Haldorsen, 1981; Hooke and Iverson, 1995). Dreimanis and Vagners (1971, 1972) observed that there is a comminution threshold, or terminal grade, at which sediment grains are not reduced beyond a particular size, even with continued subglacial transport. The terminal grade is likely controlled by a minimum fracture length that is influenced by the presence of microcracks, the sizes of crystals, and mineral hardnesses (e.g., Barenblatt, 1962; Dreimanis and Vagners, 1971). When a clast is reduced below the terminal grade, fracturing does not continue and comminution ceases. Each mineral has its own terminal grade (Dreimanis and Vagners, 1971; 1972).

The terminal grades of feldspars, amphiboles, pyroxenes, and heavy minerals are between ~30 and 63 μm (Dreimanis and Vagners, 1972). The terminal grain sizes of quartz and carbonate

minerals contain "major" modes in this coarse silt fraction, though their terminal grades extend to 4 μm (Dreimanis and Vagners, 1972). Feldspars are the predominant mineral of Earth's continental crust, and heavy minerals dominate the rare earth element concentrations and thus the εNd of silts and sand-sized sediments (e.g., Garcon et al., 2014). Accordingly, the coarse silt fraction (30-63 μm) of glacigenic sediments increases with transport distance and contains the mineral assemblage that is mixed through comminution and transport along the ice stream path. Heavy minerals would be comminuted to the terminal grade after approximately 80 to 180 kilometers of transport at the glacial bed, with less transport being necessary for comminution to the terminal grade among the less resistant minerals (Dreimanis and Vagners, 1971). Therefore, heterogeneities in the εNd of fine glacigenic sediments are minimized by the long transport distances required for terminal comminution of heavy minerals.

2. Materials and Methods

2.1 Glacigenic and Riverine Sediments

Modern riverine sediments were collected from the estuaries and lagoons of various rivers draining into the Baltic and Bothnian Sea basins (Table 1; Fig. 1; Toucanne et al., 2015). Rivers of the western and northern Baltic basin, including the Umealven, Lulealven, Kiiminkijoki, and Kymijoki, drain the widely-exposed crystalline bedrocks of the Fennoscandian Shield while the rivers of the southern and southeastern Baltic, including the Elbe, Oder, Vistula, Neman, Daugava, Gauja, and Narva, integrate the diverse Phanerozoic sedimentary rocks of the East European Platform (Table 1; Winterhalter et al., 1981; Andersson et al., 1992). The catchment of the Neva

river, with its terminus in the easternmost Gulf of Finland, includes both Precambrian and Phanerozoic basement rocks.

Glacigenic sediments from the Late Weichselian (Last Glacial) were collected from moraines, ice-marginal valleys (IMVs), and proglacial lakes along the southern margin of the Baltic Ice Stream terminus in Denmark, Germany, and Poland (Table 2; Toucanne et al., 2015). Outwash sediments from the Brandenburg-Leszno advance phase (23.4±0.3 to 20.3±0.2 ka BP, Toucanne et al., 2015) were acquired from the Głogów-Baruth IMV in Beelitz, eastern Germany (Lüghtens et al., 2010) and Karchowo and Hetmanice, western Poland (Krzyskowski et al., 1999). Tills and glacial diamicts from the Frankfurt-Poznan phase (18.7±0.3 to 18.2±0.2 ka BP) were gathered in Kozłowo, Glaznoty, Chrostkowo, and Obórki villages in eastern Poland (Wysota et al., 2009; Tylman et al., 2012; Lesemann et al., 2010; Narloch et al., 2012). Outwash plain and glaciolacustrine sediments of the Pomeranian phase (16.7±0.2 to 15.7±0.3 ka BP) were recovered from Althüttendorf and Macherslust, respectively, in the Torun-Eberswalde IMV (Lüghtens et al., 2011). Additional glaciolacustrine sediments were sourced from the Brodtener Ufer cliff exposure on the Baltic shore in Travemünde (Kabel, 1983).

In Denmark, samples were collected from cliff exposures and gravel mining pits on the islands of Sjælland and Møn. Samples from Møn were identified in consultation with the lithostratigraphy of Houmark-Nielsen (1999). From a beach cliff in Tøvelde, we procured till samples from the pre-LGM Baltic advance (Klintholm, ~35 to 30.7±0.7 ka BP; Toucanne et al., 2015), the main LGM advance (Mid-Danish), and post-LGM readvance (Young Baltic). The upper half-meter of the Klintholm till contained pronouncedly larger gravel clasts than the lower section; we sampled both. At a nearby beach cliff in Hvide, we sampled a diamict from the Kobbelgård beds that post-dates the main LGM advance and has been correlated to the Allarp till in Skåne, Sweden (Houmark-Nielsen, 1999). At a mining pit in Ledreborg, we acquired outwash sediments

from the Mid-Danish advance and till from the overlying Young Baltic advance. Mid-Danish outwash sediments were also gathered at Knarbos Klint, south of Ordrup Næs. The Mid-Danish advance is equivalent to the Brandenburg-Leszno advance in Germany and Poland, while the Young Baltic re-advances are correlative to the Frankfurt-Poznan and Pomeranian phases (Houmark-Nielsen and Kjær, 2003; Toucanne et al., 2015).

2.2 Grain size and Nd isotope analyses

The grain size distributions of the bulk glacigenic sediments were measured by laser diffractometry on an LS200 Coulter at IFREMER in Brest, France (n=23, Table S1). Samples were wet-sieved to remove gravels and then dried. Representative aliquots of the dried fractions were sonicated immediately prior to analysis to prevent clay flocculation. Volume percentages of grain size in each class (Table S1) were calculated from the mean of at least 3 replicates for each sample. We conservatively estimate the internal reproducibility of each measurement at the 1% level.

Toucanne et al. (2015) reported Nd isotope analyses performed on the <63 μm fractions of circum-Baltic river sediments and glacigenic sediments from Germany and Poland (Tables 1, 2). Here, we report Nd isotope analyses from the <63 μm fraction of glacigenic sediments from Denmark using the same procedure (Table 2). Prior to digestion by alkaline fusion (Bayon et al., 2009), organic material, carbonates, and Fe-Mn oxides were removed in the manner described by Bayon et al. (2002). Nd was then isolated by ion-exchange chromatography. All Nd isotope measurements (Toucanne et al., 2015; this study) were performed at the Pôle Spectrométrie Océan in Plouzané, France using a Thermo Scientific Neptune multi-collector ICP-MS. Nd isotopic compositions of the samples were calculated by sample-standard bracketing, with the JNdi-1 standard solution analyzed every two samples. Exponential mass-bias corrections were applied to

176 the Nd isotope ratios using $^{146}Nd/^{144}Nd = 0.7219$, and the mass-bias corrected $^{143}Nd/^{144}Nd$ values
177 were normalized to a JNdi-1 value of $^{143}Nd/^{144}Nd = 0.512115$ (Tanaka et al., 2000). The estimated
178 uncertainty of our measurements is ±0.3 ε-units (2σ) based on the external reproducibility of
179 replicate analyses of the JNdi-1 standard solution ($^{143}Nd/^{144}Nd = 0.512115 \pm 0.000009$, 2σ, n=31).
180 Procedural blanks contained 7 and 12 pg of Nd while the samples contained between 1.4×10^5 and
181 9.0×10^5 pg of Nd. We report $^{143}Nd/^{144}Nd$ ratios in εNd notation,
182 $[(^{143}Nd/^{144}Nd)_{sample}/(^{143}Nd/^{144}Nd)_{CHUR} - 1] \times 10^4$, using the $(^{143}Nd/^{144}Nd)_{CHUR}$ value of 0.512638
183 (Jacobsen and Wasserburg, 1980).
184
185 2.3 Endmember Modeling of Sedimentary Processes
186
187 Silts compose a volumetrically significant but underutilized fraction of subglacially
188 transported sediments since, due to their small size, petrographic identification of provenance is
189 ineffective. As such, we seek to infer the relative transport distances of glacigenic sediments from
190 their grain size distributions, specifically the relative concentrations of coarse silts. This strategy
191 is based on empirical observations that the proportion of coarse silt in a till increases with transport
192 distance (e.g., Dreimanis and Vagners 1971; 1972). Here, we quantitatively verify the grain size
193 signature of comminution in our samples by endmember modeling analysis (EMMA).
194 EMMA is an eigenspace method of solving the bilinear mixing problem in which the
195 number of endmembers (EMs) and their relative proportions are not known in advance (Weltje,
196 1997). EMMA explains the structure of observations in a dataset as a smaller number of non-
197 negative EMs (Dietze et al., 2012). The grain size distributions of sediments are dominated by a
198 discrete number of processes that can act to comminute and transport them. EMMA allows us to
199 discriminate individual processes operating on the sediment distributions.

To evaluate the EMs, we perform singular value decomposition on the matrix of our grain size data and obtain the characteristic eigenvalues and eigenvectors following the method of Dietze et al. (2012). Each eigenvalue is paired to an eigenvector, and the normalized eigenvalues correspond to the percentage of variance in the data explained by the associated eigenvector. In practice, only a few eigenpairs are relevant because they explain most of the variance in the dataset. The selected eigenvectors are rotated orthogonally following the method of Kaiser (1958) and normalized. The EM scores, corresponding to the relative proportions of each EM in the grain size distributions, are estimated by least squares with non-negativity constraints (as introduced by Lawson and Hanson, 1974) from the grain size data matrix and the rotated and normalized eigenvectors. Lastly, the EMs are defined by rescaling the rotated and normalized eigenvectors to non-negative percentages such that each sums to 100% (Dietze et al., 2012).

To test whether the number of studied grain size distributions is enough to have certainty in our EMs, we resample the data with replacement, known as the bootstrap method (i.e., Efron and Tibshirani, 1994). For 1000 bootstrap samples, the EMMA was performed on 23 randomly selected grain size distributions with replacement allowing for the same distribution to be chosen multiple times per bootstrap.

3. Results

3.1 Grain Sizes

The grain size distribution data obtained for this study are reported in Table S1. The proportion of subglacially transported sediment in each glacigenic sample is estimated from the relative abundances of coarse silt within the silt and clay fraction (30-63 μm / <63 μm). We term

this ratio the comminution index. The comminution indices of the glaciolacustrine samples cluster between 0.12 and 0.24 (Table 2). The till and diamict samples range from 0.14 to 0.36. There is greater variability in the comminution indices of the glacial outwash deposits, from 0.10 to 0.64.

3.2 Neodymium Isotopes

The εNd of the glacigenic sediments from Denmark are reported in Table 2 (n=8). The εNd of these samples range from -16.4 to -14.9. For comparison, Toucanne et al. (2015) reported εNd of glacigenic sediments from Germany and Poland between -16.5 and -12.4 (n=15, Table 2). From the εNd of terrigenous river sediments that drain into the Baltic and Bothnian Seas (Table 1), we document an approximately north-south trend (R^2=0.83, $p < 10^{-5}$) in the formation age of exposed Fennoscandian crust (Fig. 2). Prediction intervals (95%) for the trendline in Fig. 2 are calculated by bootstrapping of the observations with replacement (n=1000).

3.3 Model Endmembers

We perform EMMA on the grain size distributions of the glacigenic sediments (n=23). We restrict our domain of consideration to particles between 2 and 125 μm because we are focusing on the processes that affect fine sediment size distributions. The EMMA identifies 3 EMs that can be mixed to explain 97% of variance in the data, satisfying a common criterion for EM selection (>95%, e.g., Reyment and Joreskog, 1993). The first EM is predominantly composed of fine silt grains (79% ≤ 16 μm). The second EM mainly consists of medium and coarse silts (68% 16-63 μm). The third EM is mostly fine sand (51% 63-125 μm) and fine silt (31% ≤ 16 μm), but lacks medium and coarse silt (18% 16-63 μm). The robustness of the model is verified by bootstrapping

248 the 95% confidence intervals for each EM (Fig. 3) and by ensuring that the form of the EMs is
249 insensitive to the specific choice of grain size domain boundaries.
250
251 4. Discussion
252
253 4.1 Transport and Sorting Processes
254
255 Each of the three EMs appears to represent a different set of processes. We interpret the
256 first EM to represent the concentration of fine silts that have been sorted hydraulically through
257 glaciofluvial and lacustrine processes. The first EM scores highly for all of the glaciolacustrine
258 and two of the outwash sediments. The tills from eastern Denmark also have elevated scores for
259 the first EM, consistent with their incorporation of chalk, limestone, and sandy marl substrata (i.e.,
260 Houmark-Nielsen, 2003). The second EM has a pronounced mode in the terminal grain sizes of
261 heavy minerals and feldspar, exhibiting characteristics of the comminution process (Dreimanis and
262 Vagners, 1972). The third EM appears to characterize a poorly-sorted till that lacks medium and
263 coarse silts that would have been concentrated by comminution (EM 2). Our interpretation is
264 consistent with the third EM scoring highly for the German and Polish till samples and at low
265 values for each of the glaciolacustrine sediments (Table 2).
266 We suspect that some of the glaciolacustrine and outwash sediments (Table 2) experienced
267 significant post-transport sorting by water. Such sorting would alter the grain size proxy and
268 possibly change the amount and concentration of the heavy minerals that control the εNd. We
269 compare the proportions of coarse silt and fine sand (30-125 μm / <125 μm) in the glaciolacustrine
270 and outwash sediments to the average of our German and Polish tills (0.48 ± 0.06 μm, 1σ) to
271 quantify the relative sorting of these samples. All four glaciolacustrine sediments (from 0.13 to

0.29 μm) and two outwash sediments (0.11 and 0.18 μm) show depletion of coarse silt and fine sand relative to the German and Polish till deposits (Table 2). These six samples are likewise depleted in the third EM and enriched in the first EM. In contrast to the other outwash samples, the two outwash samples with low 30-125 μm / <125 μm ratios (Althüttendorf-b and Beelitz-a) also have low scores for both EMs 2 (comminuted sediments) and 3 (washed-out till). Accordingly, we do not consider these six samples in the determination of sediment transport distance by coupled εNd and grain size analyses (Sec. 4.2).

4.2 Sediment Transport from Coupled εNd and Grain Size Analyses

To calculate distances of subglacial sediment transport, we determine proxy measures for both the mean transport distance of a glacigenic sample and the proportion of sediments in the sample that were transported subglacially. The proportion of subglacially transported sediment in the sample is estimated from the relative abundances of coarse silts in the silt and clay fraction (the comminution index). Because εNd provides a robust geographic fingerprint for the origin of sediments (Sec. 1.1), the mean distance of transport, for all sediments in the sample, is estimated from the difference between the εNd of a glacigenic sample and the εNd of non-glacigenic sediments in the region where the glacigenic sample was collected. We quantify this difference as ΔεNd. Calculating ΔεNd in this manner corrects for the longitudinal variation in εNd across the Northern European Lowlands (i.e., Toucanne et al., 2015), allowing us to project our samples onto a common transport path (Figs. 1 and 4). The ΔεNd is translated into a transport distance via the relationship between the εNd and latitude of terrigenous sediments from rivers that drain into the Baltic and Bothnian Seas (R^2=0.83, Fig. 2). From this relationship, we discern that each ε-unit in the ΔεNd corresponds to ~160 km of transport in the north-south sense. For samples collected in

Germany and Poland, the regional εNd signature is measured from the river sediments of major catchments (Table 1). No comparable river system exists in Denmark, however. Therefore, for the samples collected in Denmark, we estimate the regional εNd signature (-14.3) from the y-intercept of the linear regression of Danish sample εNd values and comminution indices (i.e., Fig. 4).

To examine the relationship between the sediment transport distance and grain size, we plot the ΔεNd of each sample versus its comminution index (Fig. 4). A linear trend is fit to the data that we infer to define a mixing line between two EMs. The two EMs are the comminuted and non-comminuted fractions of the sediments, whose comminution indices are one and zero, respectively. The comminuted EM (CI=1) represents far-transported sediments whereas the non-comminuted EM (CI=0) represents sediments that were entrained near the terminal margin and therefore not comminuted to the terminal grade before deposition. By excluding the six samples described as hydraulically sorted in Sec. 4.1, we find a strong correlation (R^2=0.78, $p < 10^{-5}$) between the ΔεNd of our glacigenic sediments and their comminution indices (Fig. 4; n=17). The linear correspondence between ΔεNd and the comminution index is consistent with mixing between two well-defined EMs having similar Nd concentrations. The distal EM (CI=0) is composed of fine silts and clays with a ΔεNd value of -0.2 ± 0.7 (95% prediction interval)**.** The far-transported EM (CI=1) is composed of coarse silts and has a ΔεNd value of 5.4 (asymmetric 95% prediction interval from 3.9 to 6.5). The prediction intervals (95%) are calculated by bootstrapping with replacement (Fig. 4, n=1000).

By assuming that the Baltic Ice Stream flowed nearly along lines of longitude, a reasonable approximation to its flow path (e.g., Kleman et al., 1997; Boulton et al., 2001; Patton et al., 2016; Fig. 1), the ΔεNd indicates the source region of our samples in a simple north-south sense (Fig. 2). From the ΔεNd of the comminuted EM (CI=1), we estimate that the comminuted fractions of our sediments were deposited 850 ± 250 km (95% confidence) from their source region (Fig. 1). The

uncertainty estimate for this transport distance accounts for the analytical uncertainty of the εNd analyses for both the glacigenic and river sediments, the prediction uncertainty in ΔεNd for the comminuted EM (CI=1, Fig. 4), and the prediction uncertainties about the trendline between river εNd and latitude (Fig. 2). Because the ΔεNd of our samples are normalized to a common region of deposition at the ice sheet margin, we calculate the inferred source region of the comminuted sediments from a projected site of deposition at 53.7°N, 20°E (Fig. 1).

4.3 Sediment Sources

The inferred transport distance of 850 ± 250 km suggests that the main source of sediment erosion was most likely located near the Åland sill between the Bothnian and Baltic Seas (Fig. 1). The extensive glacial scouring and till removal in this region indicates that till cover and weathered mantle overburden were eroded in a single or a few successive glacial cycles, providing a supply of sediments for subglacial transport (Kleman et al., 2008). Consistent with this interpretation, previous researchers have documented the transport of large clasts from the northern Baltic by the LGM Baltic Ice Stream (e.g., Overweel, 1977; Houmark-Nielsen, 1987; Smed, 1993). Furthermore, our determination of a main erosion source near the Åland sill is in agreement with numerical results of Patton et al. (2016) who show a potential zone of maximum erosion here. Although the mean εNd values of the glacigenic silts are dominated by non-comminuted sediments that reflect a southern Baltic source (Toucanne et al., 2015), we demonstrate that the signature of subglacial erosion and transport can be extracted by coupling grain size and εNd analyses.

The Baltic Ice Stream advanced over the zone of maximum erosion at least twice before reaching its final LGM terminus position (Hughes et al., 2016), providing subglacially eroded sediments that could be entrained englacially (Hambrey et al., 1997; Alley et al., 1997) and

transported to the ice margin. We consider that rapid ice flow into the Baltic basins is responsible for the long transport distances of the comminuted sediments (i.e., Clark, 1987), a scenario that is supported by empirical and numerical demonstrations of rapid Fennoscandian Ice Sheet growth in the lead up to the LGM (Hughes et al., 2016; Patton et al., 2016).

In terms of its future application, the methodology introduced here could be used to infer the distances of sediment transport by other LGM ice streams, particularly those of the Laurentide Ice Sheet given the geometric similarities of its continental shield bedrock to the Baltic Ice Stream (i.e., Stokes and Clark, 2003; Stokes et al., 2016). We speculate that the most fruitful application of our method, however, would be to older glaciations, as geomorphological evidence of subglacial erosion is increasingly obscured and boundary conditions for numerical models are increasingly uncertain prior to the Last Glacial Period. As evidenced by the distribution of tills and outwash sediments in Fig. 4, future studies should take care to collect glacigenic sediments with diverse concentrations of coarse silt to ensure that mixing lines, should they exist, can be fit robustly. Furthermore, we note that our method is unlikely to be appropriate for understanding glacial processes and sediment transport at scales of tens of kilometers or less. The robustness of the relationship between the $\Delta\varepsilon Nd$ of our glacigenic sediments and their comminution indices (Fig. 4) evinces a regional homogenization of εNd in the silt and clay fractions due to the long distances of transport required for the comminution of heavy minerals to their terminal grade. To infer the transport distances of glacigenic sediments at shorter scales, researchers would be well-advised to track spatial trends in the concentration of distinctive rock fragments or metals (i.e., Hooke et al., 2013). The applicability of such dispersal train methods is limited at great lengths, however, by exponential decreases in the concentration of target rocks and metals with distance (i.e., Clark et al., 1987). An exponential relationship between $\Delta\varepsilon Nd$ and distance is not discerned in the present

study, likely because our method measures the integrated entrainment of sediments along lines of ice flow instead of erosion from a point source.

5. Conclusion

In this manuscript, we present a methodology for estimating the transport distance of fine subglacial sediments. We determine proxy measures for the mean transport distance of fine sediments in a sample as well as the proportion of the sediments that were transported subglacially. The proportion of subglacially transported sediment in a sample is estimated from the relative abundances of coarse silt in the silt and clay fraction. The conceptual basis for using grain size ratios to quantify transport is provided by empirical studies of subglacial comminution and the resulting grain size signatures. The mean distance of transport for the silts is estimated from the difference between the εNd value of the glacigenic sediment and the regional εNd signature that corresponds to the locale in which the former was collected (ΔεNd). A relationship between the εNd and latitude of circum-Baltic river sediments provides a calibrated framework for translating the ΔεNd into transport distances along lines of ice flow. Endmember modeling analysis reveals the signature of comminution in the studied sediments, validating the methodology.

We determine that the comminuted silt fractions of glacigenic sediments from the LGM terminal margin in Denmark, Germany, and Poland originated at least 850 ± 250 km to the north. This result is consistent with a main erosion source near the Åland sill and rapid ice flow into the Baltic and Bothnian Sea basins in the lead up to the LGM.

388 Acknowledgements

389

390 The authors are grateful to Jerry McManus and Doug Martinson for their feedback on early
391 versions of this manuscript. The corresponding author was introduced to the sampling localities in
392 Denmark through field trips organized by Michael Houmark-Nielsen. Angelique Roubi and
393 Mickael Rovere are thanked for their assistance with the grain size analyses. Mathilde Pitel-
394 Roudaut drafted the first figure with digitized lineation and model output files that were graciously
395 supplied by Henry Patton and Alun Hubbard. Germain Bayon generously provided guidance,
396 technical assistance, and materials for the sample preparation and chromatography. This study was
397 supported by the Climate Center, endowed by the G. Unger Vetlesen Foundation, and the Office
398 for Science and Technology of the Embassy of France in the United States.

399 References

400

401 Alley, R.B., Cuffey, K.M., Evenson, E.B., Strasser, J.C., Lawson, D.E., and Larson, G.J., 1997.
402 How glaciers entrain and transport basal sediment: physical constraints. *Quat. Sci. Rev.*, *16*(9),
403 1017-1038. doi: http://dx.doi.org/10.1016/S0277-3791(97)00034-6

404

405 Andersson, P.S., Wasserburg, G.J. and Ingri, J., 1992. The sources and transport of Sr and Nd
406 isotopes in the Baltic Sea. *Earth Planet. Sci. Lett.*, *113*(4), 459-472. doi:
407 https://doi.org/10.1016/0012-821X(92)90124-E

408

409 Asch, K., 2005. IGME 5000: 1 : 5 Million International Geological Map of Europe and Adjacent
410 Areas. BGR, Hannover.

411

412 Barenblatt, G.I., 1962. The mathematical theory of equilibrium cracks in brittle fracture. *Adv. Appl.*
413 *Mech.*, *7*, 55-129.

414

415 Bayon, G., German, C.R., Boella, R.M., Milton, J.A., Taylor, R.N. and Nesbitt, R.W., 2002. An
416 improved method for extracting marine sediment fractions and its application to Sr and Nd isotopic
417 analysis. *Chem. Geol.*, *187*, 179-199. doi: https://doi.org/10.1016/S0009-2541(01)00416-8

418

419 Bayon, G., Barrat, J.-A., Etoubleau, J., Benoit, M., Revillon, S., and Bollinger, C., 2009.
420 Determination of rare earth elements, Sc, Y, Zr, Ba, Hf and Th in geological samples by ICP-MS
421 after Tm addition and alkaline fusion. *Geostand. Geoanal. Res.*, *33*, 51-62. doi: 10.1111/j.1751-
422 908X.2008.00880.x

Bayon, G., Toucanne, S., Skonieczny, C., André, L., Bermell, S., Cheron, S., Dennielou, B., Etoubleau, J., Freslon, N., Gauchery, T., and Germain, Y., 2015. Rare earth elements and neodymium isotopes in world river sediments revisited. *Geochim. Cosmochim. Acta, 170*, 17-38. doi: http://dx.doi.org/10.1016/j.gca.2015.08.001

Bennett, M.R., 2003. Ice streams as the arteries of an ice sheet: their mechanics, stability and significance. *Earth-Sci. Rev.*, *61*(3), 309-339. doi: http://dx.doi.org/10.1016/S0012-8252(02)00130-7

Boulton, G.S., Dongelmans, P., Punkari, M., and Broadgate, M., 2001. Palaeoglaciology of an ice sheet through a glacial cycle: the European ice sheet through the Weichselian. *Quat. Sci. Rev.*, *20*(4), 591-625. doi: http://dx.doi.org/10.1016/S0277-3791(00)00160-8

Clark, P.U., 1987. Subglacial sediment dispersal and till composition. *J. Geol.*, *95*(4), 527-541. doi: https://doi.org/10.1086/629147

Cuffey, K.M. and Paterson, W.S.B., 2010. *The physics of glaciers*. Academic Press.

Dietze, E., Hartmann, K., Diekmann, B., IJmker, J., Lehmkuhl, F., Opitz, S., Stauch, G., Wünnemann, B., and Borchers, A., 2012. An end-member algorithm for deciphering modern detrital processes from lake sediments of Lake Donggi Cona, NE Tibetan Plateau, China. *Sediment. Geol.*, *243*, 169-180. doi: http://dx.doi.org/10.1016/j.sedgeo.2011.09.014

Dreimanis, A. and Vagners, U.J., 1971. Bimodal distribution of rock and mineral fragments in basal tills. *Till*, 237-250.

Dreimanis, A. and Vagners, U.J., 1972. The effect of lithology upon texture of till. *Research methods in Pleistocene geomorphology*, 66-82.

Efron, B. and Tibshirani, R.J., 1994. *An introduction to the bootstrap*. Chapman & Hall/CRC.

Freslon, N., Bayon, G., Toucanne, S., Bermell, S., Bollinger, C., Chéron, S., Etoubleau, J., Germain, Y., Khripounoff, A., Ponzevera, E., and Rouget, M.L., 2014. Rare earth elements and neodymium isotopes in sedimentary organic matter. *Geochim. Cosmochim. Acta*, *140*, 177-198. doi: http://dx.doi.org/10.1016/j.gca.2014.05.016

Gaál, G. and Gorbatschev, R., 1987. An outline of the Precambrian evolution of the Baltic Shield. *Precambrian Res.*, *35*, 15-52. doi: https://doi.org/10.1016/0301-9268(87)90044-1

Garçon, M., Chauvel, C., France-Lanord, C., Limonta, M., and Garzanti, E., 2014. Which minerals control the Nd–Hf–Sr–Pb isotopic compositions of river sediments?. *Chem. Geol.*, *364*, 42-55. doi: http://dx.doi.org/10.1016/j.chemgeo.2013.11.018

Gorbatschev, R. and Bogdanova, S., 1993. Frontiers in the Baltic shield. *Precambrian Res.*, *64*(1), 3-21. doi: https://doi.org/10.1016/0301-9268(93)90066-B

Goldstein, S.J. and Jacobsen, S.B., 1988. Nd and Sr isotopic systematics of river water suspended material: implications for crustal evolution. *Earth Planet. Sci. Lett.*, *87*(3), 249-265. doi: https://doi.org/10.1016/0012-821X(88)90013-1

Haldorsen, S., 1981. Grain-size distribution of subglacial till and its relation to glacial crushing and abrasion. *Boreas*, *10*(1), 91-105. doi: 10.1111/j.1502-3885.1981.tb00472.x

Hambrey, M.J., Huddart, D., Bennett, M.R., and Glasser, N.F., 1997. Genesis of 'hummocky moraines' by thrusting in glacier ice: evidence from Svalbard and Britain. *J. Geol. Soc.*, *154*(4), 623-632. doi: https://doi.org/10.1144/gsjgs.154.4.0623

Hooke, R.L. and Iverson, N.R., 1995. Grain-size distribution in deforming subglacial tills: role of grain fracture. *Geology*, *23*(1), 57-60. doi: https://doi.org/10.1130/0091-7613(1995)023<0057:GSDIDS>2.3.CO;2

Hooke, R.L., Cummings, D.I., Lesemann, J.E. Sharpe, D.R., 2013. Genesis of dispersal plumes in till. *Canadian Journal of Earth Sciences, 50*(1), 847-855. doi: https://doi.org/10.1139/cjes-2013-0018

Houmark-Nielsen, M., 1987. Pleistocene stratigraphy and glacial history of the central part of Denmark. *Bull. Geol. Soc. Den*., *36*, 1-189.

Houmark-Nielsen, M., 1999. A lithostratigraphy of Weichselian glacial and interstadial deposits in Denmark. *Bull. Geol. Soc. Den.*, *46*(1), 101-114.

494

495 Houmark-Nielsen, M. and Kjær, K.H., 2003. Southwest Scandinavia, 40-15 kyr BP:
496 palaeogeography and environmental change. *J. Quat. Sci.*, *18*(8), 769-786. doi: 10.1002/jqs.802

497

498 Hughes, A.L., Gyllencreutz, R., Lohne, Ø.S., Mangerud, J., and Svendsen, J.I., 2016. The last
499 Eurasian ice sheets–a chronological database and time-slice reconstruction, DATED-1. *Boreas*,
500 *45*(1), 1-45. doi: 10.1111/bor.12142

501

502 Jacobsen, S.B. and Wasserburg, G.J., 1980. Sm-Nd isotopic evolution of chondrites. *Earth Planet.*
503 *Sci. Lett.*, *50*(1), 139-155. doi: https://doi.org/10.1016/0012-821X(80)90125-9

504

505 Kabel, C., 1983. The Brodtener Ufer Cliff. In Ehlers, J. (Eds), *Glacial deposits in North-West*
506 *Europe*, 325-327. Balkema, Rotterdam.

507

508 Kaiser, H.F., 1958. The varimax criterion for analytic rotation in factor analysis. *Psychometrika*,
509 *23*(3), 187-200.

510

511 Kjær, K.H., Houmark-Nielsen, M., and Richardt, N. 2003. Ice-flow patterns and dispersal of
512 erratics at the southwestern margin of the last Scandinavian Ice Sheet: signature of palaeo-ice
513 streams. *Boreas*, *32*(1), 130-148. doi: 10.1111/j.1502-3885.2003.tb01434.x

514

515 Kleman, J., Hättestrand, C., Borgström, I., and Stroeven, A., 1997. Fennoscandian
516 palaeoglaciology reconstructed using a glacial geological inversion model. *J. Glaciol*. *43*(144),
517 283-299. doi: https://doi.org/10.3189/S0022143000003233

Kleman, J., Stroeven, A.P., and Lundqvist, J., 2008. Patterns of Quaternary ice sheet erosion and deposition in Fennoscandia and a theoretical framework for explanation. *Geomorphology*, *97*(1), 73-90. doi: http://dx.doi.org/10.1016/j.geomorph.2007.02.049

Krzyszkowski, D., Gizler, H., Jodlowski, J. and Dobosz, T., 1999. Glacial deposits and geomorphology in the zone of the maximum extent of the Weichselian ice sheet between Sława Śląska and Święciechowa, western Poland. *Quaternary Studies in Poland*, *16*, 47-66.

Lawson, C.L. and Hanson, R.J., 1974. *Solving least squares problems* (Vol. 161). Prentice-Hall, Englewood Cliffs, NJ.

Lesemann, J.E., Piotrowski, J.A. and Wysota, W., 2010. "Glacial curvilineations": New glacial landforms produced by longitudinal vortices in subglacial meltwater flows. *Geomorphology*, *120*(3-4), 153-161. doi: https://doi.org/10.1016/j.geomorph.2010.03.020

Lüghtens, C., Krbetschek, M., Böse, M. and Fuchs, M.C., 2010. Optically stimulated luminescence dating of fluvioglacial (sandur) sediments from north-eastern Germany. *Quat. Geochronol.*, *5*, 237-243. doi: https://doi.org/10.1016/j.quageo.2009.06.007

Lüghtens, C., Böse, M. and Preusser, F., 2011. Age of the Pomeranian ice-marginal position in northeastern Germany determined by Optically Stimulated Luminescence (OSL) dating of glaciofluvial sediments. *Boreas*, *40*(4), 598-615. doi: 10.1111/j.1502-3885.2011.00211.x

McLennan, S.M. and Hemming, S., 1992. Samarium/neodymium elemental and isotopic systematics in sedimentary rocks. *Geochim. Cosmochim. Acta*, *56*(3), 887-898. doi: https://doi.org/10.1016/0016-7037(92)90034-G

Mykkeltveit, S., Husebye, E.S. and Oftedahl, C., 1980. Subduction of the Iapetus ocean crust beneath the Møre gneiss region, southern Norway. *Nature*, *288*, 473-475. doi: 10.1038/288473a0

Narloch, W., Piotrowski, J.A., Wysota, W., Larsen, N.K. and Menzies, J., 2012. The signature of strain magnitude in tills associated with the Vistula Ice Stream of the Scandinavian Ice Sheet, central Poland. *Quat. Sci. Rev.*, *57*, 105-120. doi: https://doi.org/10.1016/j.quascirev.2012.09.022

Overweel, C.J., 1977. Distribution and transport of Fennoscandinavian indicators. *Scripta Geol.*, *43*, 1-117.

Patton, H., Hubbard, A., Andreassen, K., Winsborrow, M., and Stroeven, A.P., 2016. The build-up, configuration, and dynamical sensitivity of the Eurasian ice-sheet complex to Late Weichselian climatic and oceanic forcing. *Quat. Sci. Rev.*, *153*, 97-121. doi: http://dx.doi.org/10.1016/j.quascirev.2016.10.009

Reyment, R.A. and Joreskog, K.G., 1996. *Applied factor analysis in the natural sciences*. Cambridge University Press.

564 Rignot, E., Bamber, J.L., Van Den Broeke, M.R., Davis, C., Li, Y., Van De Berg, W.J. and Van
565 Meijgaard, E., 2008. Recent Antarctic ice mass loss from radar interferometry and regional climate
566 modelling. *Nat. Geosci.*, *1*, 106-110. doi: 10.1038/ngeo102
567
568 Soulet, G., Ménot, G., Bayon, G., Rostek, F., Ponzevera, E., Toucanne, S., Lericolais, G., and
569 Bard, E., 2013. Abrupt drainage cycles of the Fennoscandian Ice Sheet. *Proc. Natl. Acad. Sci.*
570 *U.S.A.*, *110*(17), 6682-6687. doi: https://doi.org/10.1073/pnas.1214676110
571
572 Stokes, C.R. and Clark, C.D., 2003. Laurentide ice streaming on the Canadian Shield: A conflict
573 with the soft-bedded ice stream paradigm?. *Geology*, *31*(4), 347-350. doi:
574 https://doi.org/10.1130/0091-7613(2003)031<0347:LISOTC>2.0.CO;2
575
576 Stokes, C.R., Tarasov, L., Blomdin, R.L., Cronin, T.M., Fisher, T.G., Gyllencreutz, R.,
577 Hättestrand, C., Heyman, J., Hindmarsh, R.C.A., Hughes, A., Jakobsson, M., Kirchner, N.,
578 Livingstone, S.J., Margold, M., Murton, J.B., Noormets, R., Peltier, W.R., Peteet, D.M., Piper,
579 D.J.W., Preusser, F., Renssen, H., Roberts, D., Roche, D.M., Saint-Agne, F., Stroeven, A.P., and
580 Teller, J.T., 2015. On the reconstruction of palaeo-ice sheets: recent advances and future
581 challenges. *Quat. Sci. Rev.*, *125*, 15-49. doi: http://dx.doi.org/10.1016/j.quascirev.2015.07.016
582
583 Stokes, C.R., Margold, M., Clark, C.D. and Tarasov, L., 2016. Ice stream activity scaled to ice
584 sheet volume during Laurentide Ice Sheet deglaciation. *Nature*, *530*, 322-326. doi:
585 10.1038/nature16947
586

Smed, P., 1993. Indicator studies: a critical review and a new data-presentation method. *Bull. Geol. Soc. Den.*, *40*, 332-344.

Stroeven, A.P., Hättestrand, C., Kleman, J., Heyman, J., Fabel, D., Fredin, O., Goodfellow, B.W., Harbor, J.M., Jansen, J.D., Olsen, L., Caffee, M.W., Fink, D., Lundqvist, J., Rosqvist, G.C., Strömberg, B., Jansson, K.N., 2016. Deglaciation of Fennoscandia. *Quat. Sci. Rev.*, *147*, 91-121. doi: https://doi.org/10.1016/j.quascirev.2015.09.016

Tanaka, T., Togashi, S., Kamioka, H., Amakawa, H., Kagami, H., Hamamoto, T., Yuhara, M., Orihashi, Y., Yoneda, S., Shimizu, H. and Kunimaru, T., 2000. JNdi-1: a neodymium isotopic reference in consistency with LaJolla neodymium. *Chem. Geol.*, *168*(3), 279-281. doi: https://doi.org/10.1016/S0009-2541(00)00198-4

Taylor, S.R. and McLennan, S.M., 1985. *The continental crust: its composition and evolution.* Blackwell Scientific Pub., Palo Alto, CA.

Toucanne, S., Soulet, G., Freslon, N., Jacinto, R.S., Dennielou, B., Zaragosi, S., Eynaud, F., Bourillet, J.F., and Bayon, G., 2015. Millennial-scale fluctuations of the European Ice Sheet at the end of the last glacial, and their potential impact on global climate. *Quat. Sci. Rev.*, *123*, 113-133. doi: http://dx.doi.org/10.1016/j.quascirev.2015.06.010

Tylman, K., Piotrowski, J.A. and Wysota, W., 2013. The ice/bed interface mosaic: deforming spots intervening with stable areas under the fringe of the Scandinavian Ice Sheet at Sampława, Poland. *Boreas*, *42*(2), 428-441. doi: 10.1111/j.1502-3885.2012.00294.x

611

612 Weltje, G.J., 1997. End-member modeling of compositional data: numerical-statistical algorithms
613 for solving the explicit mixing problem. *Math. Geol.*, *29*(4), 503-549. doi:
614 https://doi.org/10.1007/BF02775085

615

616 Winsborrow, M.C.M., Andreassen, K., Corner, G.D., and Laberg, J.S., 2010. Deglaciation of a
617 marine-based ice sheet: Late Weichselian palaeo-ice dynamics and retreat in the southern Barents
618 Sea reconstructed from onshore and offshore glacial geomorphology. *Quat. Sci. Rev.*, *29*, 424-442.
619 doi: http://dx.doi.org/10.1016/j.quascirev.2009.10.001

620

621 Winterhalter, B., Flodén, T., Ignatius, H., Axberg, S., and Niemistö, L., 1981. Geology of the
622 Baltic Sea, in: *The Baltic Sea*, A. Voipio, 1-121, Elsevier, Amsterdam, 1981. doi:
623 https://doi.org/10.1016/S0422-9894(08)70138-7

624

625 Wysota, W., Molewski, P. and Sokolowski, R.J., 2009. Record of the Vistula ice lobes in the Late
626 Weichselian glacial sequence in north-central Poland. *Quat. Int.*, *207*(1-2), 26-41. doi:
627 https://doi.org/10.1016/j.quaint.2008.12.015

628 Figure 1

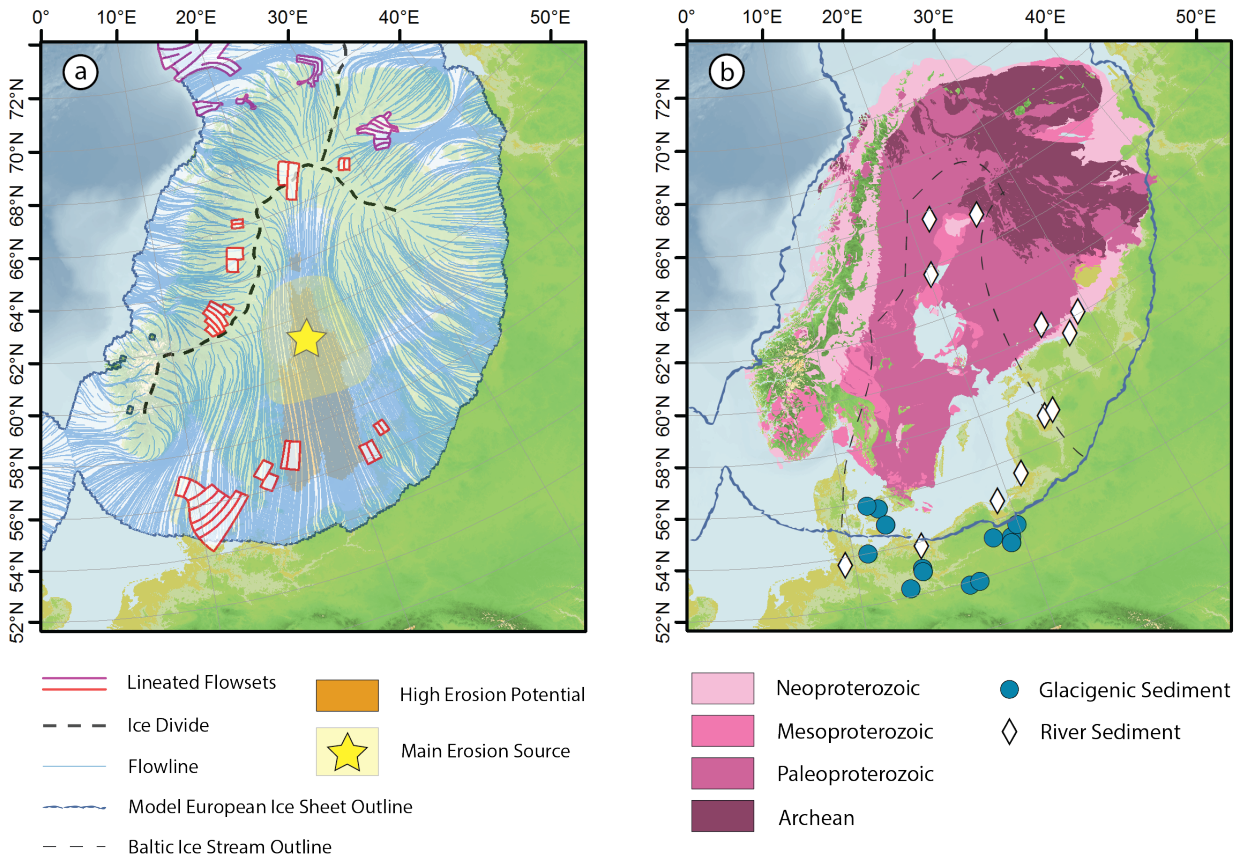

629

630

631 (a) Modeled FIS flowlines, consistent with lineated flow sets (Kleman et al., 1997; Winsborrow et
632 al., 2001), and a zone of high erosion potential (orange) beneath the Baltic Ice Stream (Patton et
633 al., 2016). The main source of erosion for the sediments considered in this study (Sec. 4.3) is
634 indicated by the yellow star (Fig. 4, projected here onto the 20°E line of longitude), with 95%
635 uncertainty bounds (yellow highlight). (b) Archean and Proterozoic bedrock geology of
636 Fennoscandia (Asch, 2005), with the sampling locations of the riverine (Table 1) and glacigenic
637 (Table 2) sediments discussed in this manuscript. Note that the limits of the modeled FIS at 20.58
638 ka BP do not align exactly with the empirical LGM limits in the Northern European Lowlands
639 (Patton et al., 2016).

640 Figure 2

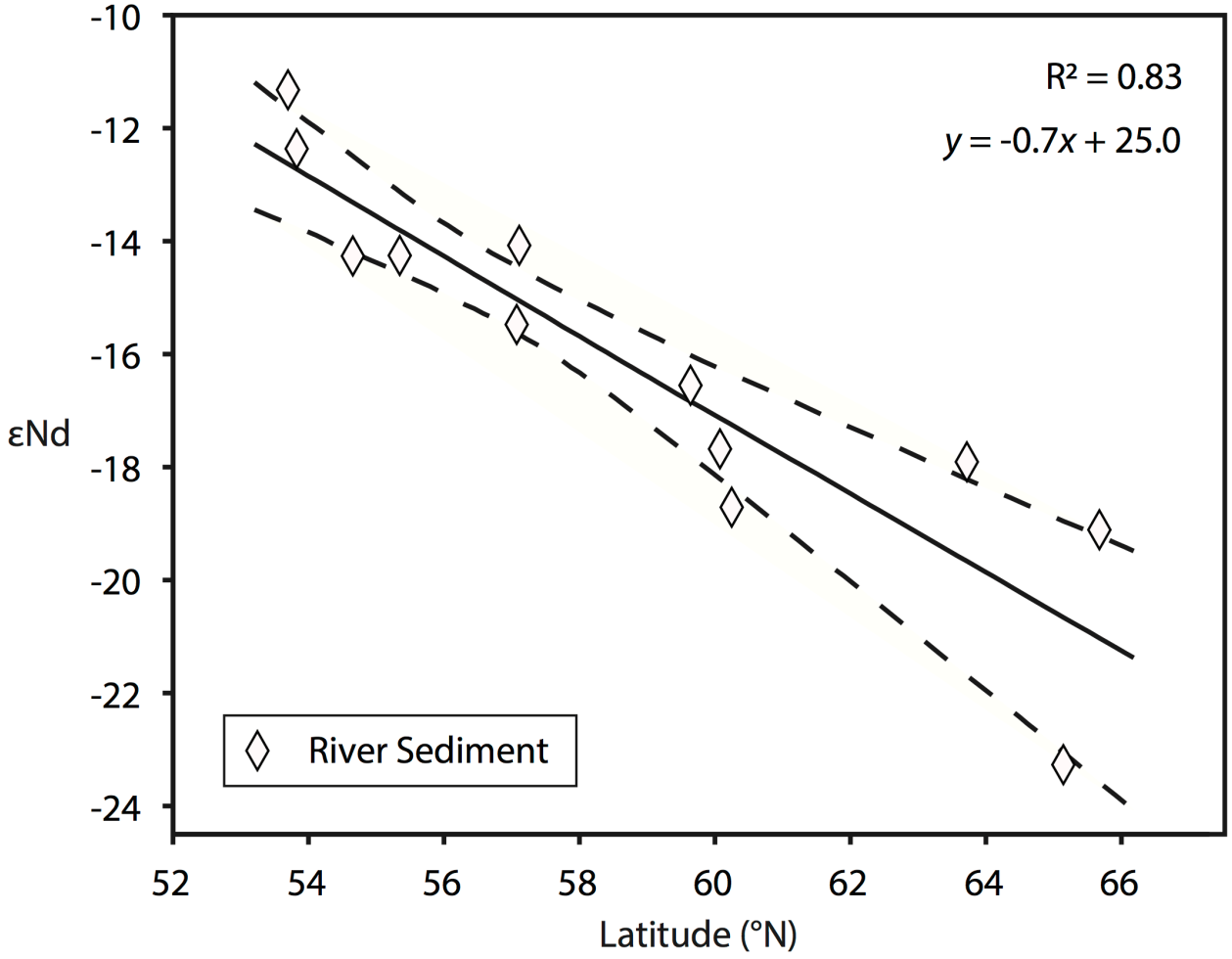

641

642

643 The latitudinal distribution and εNd of circum-Baltic river sediments (Fig. 1; Table 1). The linear
644 trendline indicates that the Nd isotopes of circum-Baltic sediments, a measure of continental crust
645 formation age, are increasingly non-radiogenic (older) towards the north. This reflects the
646 distribution of Proterozoic and Archean bedrock in Fennoscandia (Fig. 1; Gaal and Gorbatschev,
647 1987). For reference, the global average εNd of suspended river loads, approximating the εNd of
648 the upper continental crust, is -10.4 (Goldstein & Jacobsen, 1988). The trendline and its 95%
649 prediction interval (dashed lines) were calculated by bootstrapping.

650 Figure 3

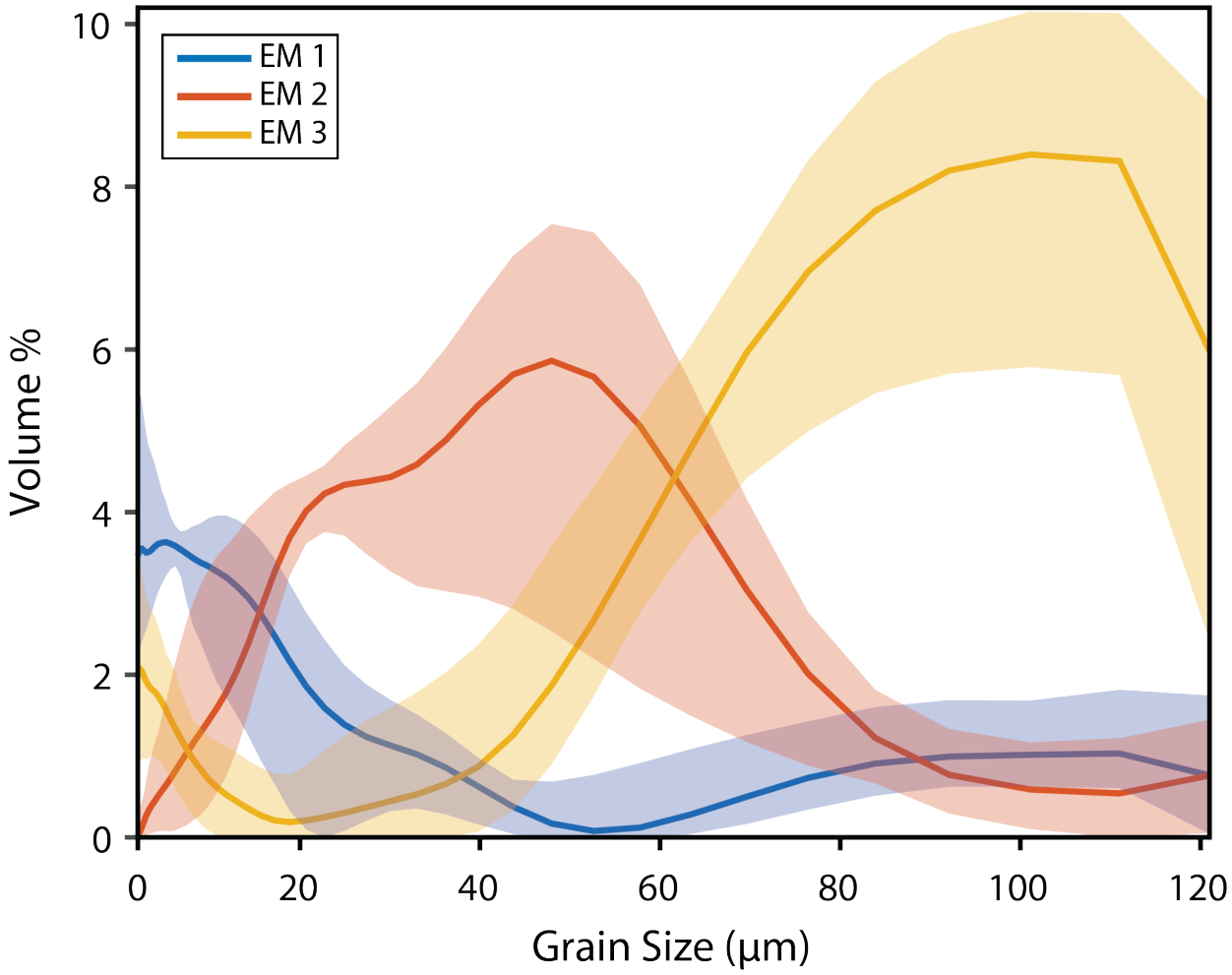

651

652

653 The three EMs determined by endmember modeling analysis. The EMs represent independent
654 processes controlling the grain size distributions of the glacigenic sediments. EM 1 illustrates the
655 concentration of fine-grained sediments by glaciofluvial and lacustrine sorting, EM 2 is the
656 comminution process of Dreimanis & Vagners (1971; 1972), and EM 3 represents a poorly sorted,
657 washed-out till distribution. Confidence intervals (95%) about the EMs were determined by
658 bootstrapping.

Figure 4

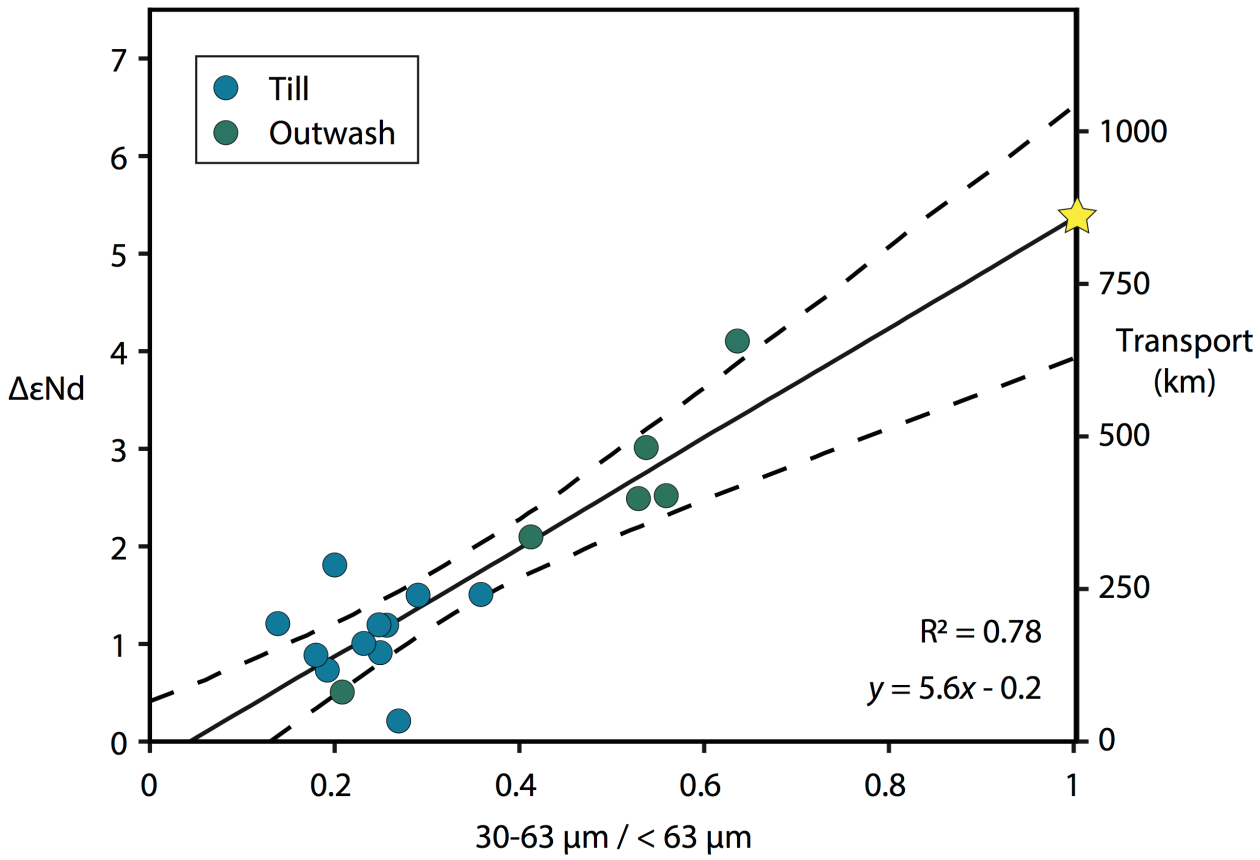

ΔεNd (the difference between the εNd of the glacigenic sediment and εNd signature of the catchment in which the sample was collected) vs. the comminution index (the proportion of glacigenic modification) of the glacigenic samples. The fully comminuted endmember (CI=1) is represented by the yellow star (projected onto a common line of longitude bisecting the Baltic Sea in Fig. 1). This endmember reveals that the main geographical origin of the subglacially-transported sediments have an Nd isotope signature that is 5.4 ε-units less radiogenic (older, more northward in this case) than the locale they were recovered from. The trendline and its 95% prediction interval (dashed lines) were calculated by bootstrapping. Transport distance is inferred from ΔεNd per the relationship in Fig. 2. The locations of the tills (blue) and outwash sediments (green) are displayed in Fig. 1.

672 Table 1

River	Country	Latitude (°N)	Longitude (°E)	εNd ± 2σ
Elbe	Germany	53.703	9.449	-11.3 ± 0.3
Oder	Poland	53.841	14.121	-12.4 ± 0.3
Vistula	Poland	54.651	19.287	-14.3 ± 0.3
Neman	Lithuania	55.362	21.257	-14.3 ± 0.3
Daugava	Latvia	57.060	24.039	-15.5 ± 0.3
Gauja	Latvia	57.133	24.684	-14.1 ± 0.3
Narva	Estonia	59.489	28.040	-16.4 ± 0.3
Neva	Russia	60.070	29.279	-17.7 ± 0.3
Kymijoki	Finland	60.260	26.496	-18.7 ± 0.3
Kiiminkijoki	Finland	65.133	25.731	-23.3 ± 0.3
Lulealven	Sweden	65.682	21.820	-19.1 ± 0.3
Umealven	Sweden	63.718	20.267	-17.9 ± 0.3

673

674

675 Information for the circum-Baltic river sediments considered in this project, compiled from
676 Toucanne et al. (2015), Freslon et al. (2014), and Soulet et al. (2013). The locations of the
677 sediments are displayed in Fig. 1. The estimated uncertainty of the measurements is ±0.3 ε-units
678 (2σ) based on the external reproducibility of replicate analyses of the JNdi-1 standard solution
679 (Toucanne et al., 2015).

Table 2

Sample	Lat. (°N)	Lon. (°E)	Type	Regional (εNd)	Sample (εNd)	ΔεNd	30-63 / < 63 µm	30-125 / < 125 µm	EM 1 Score	EM 2 Score	EM 3 Score
Althüttendorf-a	52.963	13.872	Outwash	Oder (-12.4)	-16.5	4.1	0.64	0.83	0	23	77
Althüttendorf-b*	52.963	13.872	Outwash	Oder (-12.4)	-15.7	3.3	0.11	0.11	62	38	0
Travermünde S1*	53.971	10.883	Glaciolac.	Elbe (-11.3)	-12.4	1.1	0.21	0.28	46	54	0
Travermünde S5*	53.971	10.883	Glaciolac.	Elbe (-11.3)	-14.2	2.9	0.24	0.29	33	67	0
Macherslust-a*	52.848	13.838	Glaciolac.	Oder (-12.4)	-14.8	2.4	0.12	0.13	62	38	0
Macherslust-b*	52.848	13.838	Glaciolac.	Oder (-12.4)	-15.6	3.2	0.17	0.24	82	2	16
Beelitz-a*	52.288	12.937	Outwash	Elbe (-11.3)	-13.9	2.6	0.10	0.18	89	0	11
Beelitz-b	52.288	12.937	Outwash	Elbe (-11.3)	-13.8	2.5	0.53	0.57	0	100	0
Oborki	53.152	19.381	Till	Vistula (-14.3)	-16.1	1.8	0.20	0.40	37	17	47
Hetmanice ST/17	51.858	16.265	Outwash	Oder (-12.4)	-14.9	2.5	0.56	0.60	0	100	0
Karchowo ST/14	51.889	16.834	Outwash	Oder (-12.4)	-15.4	3.0	0.54	0.58	0	100	0
Kozłowo	53.341	18.341	Till	Vistula (-14.3)	-15.8	1.5	0.29	0.53	17	20	63
Glaznoty	53.535	19.904	Till	Vistula (-14.3)	-15.8	1.5	0.36	0.54	8	42	50
Chrostkowo 1	52.943	19.253	Diamict	Vistula (-14.3)	-14.5	0.2	0.27	0.49	25	19	56
Chrostkowo 2	52.943	19.253	Diamict	Vistula (-14.3)	-15.2	0.9	0.25	0.46	30	16	54
Ledreborg MD	55.626	12.046	Outwash	Denmark (-14.3)	-16.4	2.1	0.41	0.68	3	25	73
Ledreborg YB	55.626	12.046	Till	Denmark (-14.3)	-15.0	0.7	0.19	0.27	63	29	8
Ordrup MD	55.817	11.377	Outwash	Denmark (-14.3)	-14.9	0.5	0.21	0.4	37	21	42
Tøvelde KL	54.946	12.301	Till	Denmark (-14.3)	-15.4	1.0	0.23	0.29	52	48	0
Tøvelde KU	54.946	12.301	Till	Denmark (-14.3)	-15.5	1.2	0.25	0.36	42	47	11
Tøvelde MD	54.946	12.301	Till	Denmark (-14.3)	-15.5	1.2	0.14	0.22	74	21	5
Tøvelde YB	54.949	12.307	Till	Denmark (-14.3)	-15.3	0.9	0.18	0.27	59	34	7
Hvide 3	54.935	12.278	Diamict	Denmark (-14.3)	-15.5	1.2	0.26	0.45	31	24	45

Information for the glacigenic sediments considered in this project. Glaciolacustrine and select outwash sediments (indicated by an asterisk) were excluded from the provenance analysis (Sec. 4.2) based on evidence that the grain size distributions of these samples are corrupted by post-depositional sorting (Sec. 4.1). EM 1 corresponds to the concentration of fine-grained sediments by glaciofluvial and lacustrine sorting. EM 2 is the comminution process. EM 3 represents till genesis (Sec. 4.1). The εNd of sediments from Denmark are first reported in this study; those from Germany and Poland were reported by Toucanne et al. (2015). The estimated uncertainty of the measurements is ±0.3 ε-units (2σ) based on the external reproducibility of replicate analyses of the JNdi-1 standard solution (i.e., Sec. 2.2, this study; Toucanne et al., 2015). The internal precision of the Danish sediment εNd analyses ranges from 0.08 to 0.12 ε-units (2 SE).